Article:
Mahmood, MS and Lesnic, D orcid.org/0000-0003-3025-2770 (2019) Identification of conductivity in inhomogeneous orthotropic media. International Journal of Numerical Methods for Heat and Fluid Flow, 29 (1). pp. 165-183. ISSN 0961-5539

https://doi.org/10.1108/HFF-11-2017-0469

Identification of conductivity in inhomogeneous orthotropic media

Abstract

Purpose - The purpose of this paper is to solve numerically the identification of the thermal conductivity of an inhomogeneous and possibly anisotropic medium from interior/internal temperature measurements.
Design/methodology/approach - The formulated coefficient identification problem is inverse and ill-posed and therefore, in order to obtain a stable solution, a nonlinear regularized least-squares approach is employed. For the numerical discretisation of the orthotropic heat equation, the finite-difference method is applied, whilst the nonlinear minimization is performed using the MATLAB toolbox routine **lsqnonlin**.
Findings - Numerical results show the accuracy and stability of solution even in the presence of noise (modelling inexact measurements) in the input temperature data.
Research limitations/implications - The mathematical formulation uses temporal temperature measurements taken at many points inside the sample and this may be too much information that is provided to identify a spacewise dependent only conductivity tensor.
Practical implications - Since noisy data are inverted, the study models real situations in which practical temperature measurements recorded using thermocouples are inherently contaminated with random noise.
Social implications - The identification of the conductivity of inhomogeneous and orthotropic media will be of great interest to the inverse problems community with applications in geophysics, groundwater flow and heat transfer.
Originality/value - The current investigation advances the field of coefficient identification problems by generalising the conductivity to be orthotropic in addition of being heterogeneous. The originality lies in performing, for the first time, numerical simulations of inversion to find the anisotropic and inhomogeneous thermal conductivity form noisy temperature measurements. Further value and physical significance is brought in by determining the degree of cure in a resin transfer molding process, in addition to obtaining the inhomogeneous thermal conductivity of the tested material.

Keywords: Inverse problem; orthotropic and inhomogeneous media; regularization; nonlinear least-squares.

1 Introduction

Growing research activities have been taking place in the numerical techniques and computational algorithms for solving inverse problems in different fields such as biomedical, see e.g. Paruch (2017), and heat transfer, see e.g. Yan *et al.* (2015), Alifanov (2017), processes. These problems involve situations in which the interior physical parameters or experimental measurements are inaccessible inside the domain or difficult to obtain accurately.

In many manufacturing applications, particularly in advanced composite material science, inverse modelling is considered as the most important stage for monitoring the structural integrity of materials, see e.g. Dawson *et al.* (2013). Accurate knowledge of thermal properties and heat transfer modelling within composite materials are crucial issues and very attractive research field, see e.g. Monchiet and Bonnet (2013). For these materials there are different types of media such as isotropic, orthotropic and anisotropic.

Identification of the thermal conductivity of a fully inhomogeneous and anisotropic medium is ill-posed in nature because it depends on indirect observable measurements which contain small errors that could result in large changes in the solution. In addition, there is the notorious issue of non-identifiability in the sense that even the full knowledge of the Dirichlet-to-Neumann boundary map is not sufficient to determine the anisotropic and inhomogeneous conductivity tensor of a material subject to steady-state heat conduction or electrostatic excitations, see Lionheart (1997). Moreover, even if in the isotropic but inhomogeneous case the conductivity can be uniquely determined from the complete knowledge of the Dirichlet-to-Neumann map, see Kohn and Vogelius (1985), this is still not so practical because an infinite number of measurements has to be performed for providing all the necessary boundary temperature/potential and heat/current flux. In order to deal with this non-identifiability issue, some previous studies, see e.g. Irmay (1980), Richter (1981), Knowles (2001), Knowles and Yan (2002), proposed to measure the dependent variable (temperature, piezometric head or electric potential) everywhere inside the solution domain such that the original second-order elliptic equation is recast as a first-order hyperbolic equation. More recently, Bal *et al.* (2014) suggested to measure many internal current densities in order to guarantee a unique and explicit reconstruction of a fully anisotropic conductivity tensor entering a steady-state Darcy flow conductivity equation. An even more engineering approach is to assume that the conductivity is constant, piecewise constant or linearly dependent on the space variables, see Hematiyan *et al.* (2015), Chen *et al.* (2016), Mustata *et al.* (2001), Lesnic *et al.* (2007) and Harris *et al.* (2008), such that a parameter finite dimensional problem is to be solved in a nonlinear least squares sense.

The paper is devoted to the simultaneous estimation of tensor components of an inhomogeneous thermal conductivity for which the functional minimization has to be performed in an infinite dimensional space of functions. The convergence is reached by iteration taking into account of temperature measurements in both space and time inside the solution domain to determine the thermal conductivity coefficient uniquely.

The paper includes seven sections. We give the mathematical formulation of the problem in section 2. The finite-difference method used to discretise the direct problem is given in section 3. Section 4 is devoted to describe the regularized nonlinear minimization used for solving in a stable manner the inverse coefficient identification problem. In Section 5, we provide numerical results and discussion. In Section 6, we present a physical example of including and identifying the degree of cure in a resin transfer molding process. Finally, conclusions are presented in Section 7.

2 Mathematical formulation

The heat flow through heat conducting media is significantly affected by their heterogeneous and/or anisotropic structure. A similar situation occurs in fluid flow through porous media. Therefore, let us consider a transient planar heat conduction problem in the bounded domain $\Omega \times (0,T]$, where $T > 0$, with continuously space varying anisotropic material properties. This problem is governed by the unsteady two-dimensional heat conduction equation for the transient temperature $u(x,y,t)$, namely,

$$C(x,y)\partial_t u - \nabla \cdot (\mathbf{K}(x,y)\nabla u) = S(x,y,t), \quad (x,y,t) \in \Omega \times (0,T], \tag{2.1}$$

where $C > 0$ is the heat capacity, S is a source term and the thermal conductivity matrix

$$\mathbf{K}(x,y) = \begin{pmatrix} k_{11}(x,y) & k_{12}(x,y) \\ k_{21}(x,y) & k_{22}(x,y) \end{pmatrix}, \tag{2.2}$$

is a continuous, symmetric and positive definite matrix, i.e. $k_{12} = k_{21}$ and $k_{11}k_{22} - k_{12}k_{21} > 0$.

The conductivity $\mathbf{K}$ can be either: isotropic ($k_{11} = k_{22}$, $k_{12} = k_{21} = 0$), orthotropic ($k_{11} \neq k_{22}$, $k_{12} = k_{21} = 0$) or anisotropic ($k_{11} \neq k_{22}$, $k_{12} = k_{21} \neq 0$). We take the space solution domain Ω be the rectangle $(0,l_1)\times(0,l_2)$ and solve the time-dependent heat equation (2.1) subject to the following Neumann heat flux boundary and initial conditions:

$$-(\mathbf{K}\nabla u)\cdot n|_{x=0} = g_1(0,y,t), \quad \text{on } y \in (0,l_2),\ t \in (0,T] \tag{2.3}$$
$$-(\mathbf{K}\nabla u)\cdot n|_{x=l_1} = g_2(l_1,y,t), \quad \text{on } y \in (0,l_2),\ t \in (0,T] \tag{2.4}$$
$$-(\mathbf{K}\nabla u)\cdot n|_{y=0} = g_3(x,0,t), \quad \text{on } x \in (0,l_1),\ t \in (0,T] \tag{2.5}$$
$$-(\mathbf{K}\nabla u)\cdot n|_{y=l_2} = g_4(x,l_2,t), \quad \text{on } x \in (0,l_1),\ t \in (0,T] \tag{2.6}$$

$$u(x,y,0) = u_0(x,y), \qquad (x,y) \in \overline{\Omega} \tag{2.7}$$

where $(g_i)_{i=\overline{1,4}}$ are prescibed heat flux functions, $n = (n_x, n_y)$ is the outward unit normal vector to the boundary $\partial\Omega$, and the co-normal derivative is given by

$$-(\mathbf{K}\nabla u)\cdot n = -(k_{11}\partial_x u + k_{12}\partial_y u, k_{21}\partial_x u + k_{22}\partial_y u)\cdot(n_x, n_y).$$

This Neumann model for isotropic media with thermal conductivity $\mathbf{K}(x,y,t)$ depending also on the time variable has been solved by Huang and Chin (2000) using the conjugate gradient method (CGM). In contrast to that problem, our formulation considers the identification of the time-independent but orthotropic media with thermal conductivity tensor given by

$$\mathbf{K}(x,y) = \begin{pmatrix} k_{11}(x,y) & 0 \\ 0 & k_{22}(x,y) \end{pmatrix}. \tag{2.8}$$

3 The numerical solution of the direct problem

In this section, we describe the finite-difference method (FDM) used for solving the direct problem (2.1), (2.3)-(2.8), when the thermal conductivity $\mathbf{K}$ is given. For this purpose we rewrite equation (2.1) as

$$C\partial_t u = k_{11}\partial^2_{xx}u + k_{22}\partial^2_{yy}u + \partial_x k_{11}\partial_x u + \partial_y k_{22}\partial_y u + S. \tag{3.9}$$

We start from the standard finite difference notation and discretize the computational domain $\Omega = (0, l_1) \times (0, l_2)$ into uniformly spaced grid points such that $x_i = (i-1)h_x$ and $y_j = (j-1)h_y$ for $i = 1, ..., n_x + 1, j = 1, ..., n_y + 1$, where $h_x = l_1/n_x$ and $h_y = l_2/n_y$. Let n_t be a positive integer and $t_n = n\tau$, $\tau = T/n_t$ for $n = 0, ..., n_t$. Denoting by $u^n_{i,j}$ the approximate solution $u(x_i, y_j, t_n)$, the FDM can be used to discretize the equation (3.9) as

$$C(x_i, y_j)\frac{u^{n+1}_{i,j} - u^n_{i,j}}{\tau} = (k_{11})_{i,j}\frac{u^n_{i+1,j} - 2u^n_{i,j} + u^n_{i-1,j}}{h_x^2} + (k_{22})_{i,j}\frac{u^n_{i,j+1} - 2u^n_{i,j} + u^n_{i,j-1}}{h_y^2}$$
$$+(\partial_x k_{11})_{i,j}\frac{u^n_{i+1,j} - u^n_{i-1,j}}{2h_x} + (\partial_y k_{22})_{i,j}\frac{u^n_{i,j+1} - u^n_{i,j-1}}{2h_y} + S(x_i, y_j, t_n), \quad (3.10)$$

where

$$(\partial_x k_{11})_{i,j} = \frac{(k_{11})_{i+1,j} - (k_{11})_{i-1,j}}{2h_x}, \quad (\partial_y k_{22})_{i,j} = \frac{(k_{22})_{i,j+1} - (k_{22})_{i,j-1}}{2h_y}.$$

The boundary conditions (2.3)-(2.6) and the initial condition (2.7) are approximated as

$$-(k_{11})_{1,j}\,\frac{u^{n+1}_{1,j} - u^{n+1}_{2,j}}{h_x} = g_1(0, jh_y, t_{n+1}), \quad (3.11)$$

$$-(k_{11})_{n_x+1,j}\,\frac{u^{n+1}_{n_x+1,j} - u^{n+1}_{n_x,j}}{h_x} = g_2(l_1, jh_y, t_{n+1}), \quad (3.12)$$

$$-(k_{22})_{i,1}\,\frac{u^{n+1}_{i,1} - u^{n+1}_{i,2}}{h_y} = g_3(ih_x, 0, t_{n+1}), \quad (3.13)$$

$$-(k_{22})_{i,n_y+1}\,\frac{u^{n+1}_{i,n_y+1} - u^{n+1}_{i,n_y}}{h_y} = g_4(ih_x, l_2, t_{n+1}), \quad (3.14)$$

$$u^0_{i,j} = u_0(x_i, y_j), \quad i = 1, ..., n_x + 1, \quad j = 2, ..., n_y. \quad (3.15)$$

The explicit FDM scheme (3.10) is conditionally stable, see Ozisik (1993), and the condition reads as

$$\tau\left(\frac{1}{h_x^2} + \frac{1}{h_y^2}\right)\beta \le \frac{1}{2}, \quad \beta = \max_{i=1,2}\left\{\max_{(x,y)\in\bar{\Omega}}\frac{|k_{ii}(x,y)|}{C(x,y)}\right\}. \quad (3.16)$$

We simulate the problem (2.1), (2.3)-(2.8) by taking the initial and boundary conditions (2.3)-(2.7) with data given by:

$$u_0(x, y) = 0, \quad (x, y) \in \bar{\Omega}, \quad (3.17)$$

$$g_1(0, y, t) = -1, \quad g_2(l_1, y, t) = 1, \quad g_3(x, 0, t) = -1, \quad g_4(x, l_2, t) = 1. \quad (3.18)$$

We now present below test cases for an isotropic and an orthotropic conductivity and, for simplicity, we take the source term to be absent, i.e. $S = 0$. The space increments in x and

y axes are equal $h_x = h_y = 0.1$ with $l_1 = l_2 = 1$. This gives that $n_x = n_y = 10$. Moreover, we take $T = 1$ and $n_t = 100$ which gives $\tau = 0.01$.

In the first instance we solve the direct problem (3.10)-(3.15) with isotropic heterogeneous thermal conductivity $\mathbf{K}(x, y)$ given by

$$k_{11}(x, y) = k_{22}(x, y) = \frac{1 + x + y}{12}, \quad k_{12}(x, y) = k_{21}(x, y) = 0, \tag{3.19}$$

and constant heat capacity taken, for simplicity, to be unity. It is easy to observe that our chosen mesh size $h_x = h_y = 0.1$, time step $\tau = 0.01$, $C(x, y) = 1$ and thermal conductivity (3.19) with $\beta = 1/4$ satisfy with equality the stability condition (3.16). In addition, it is sufficiently fine to ensure that any further decrease in this mesh size did not significantly affect the accuracy of the numerical results.

Figure 1 displays the contour lines of constant temperature (isotherms) at various snapshots $t \in \{0.10, 0.20, 0.40, 1.0\}$.

Next we consider an orthotropic heterogeneous medium with conductivity tensor (2.8) given by

$$k_{11}(x, y) = \frac{1 + x + y}{12}, \quad k_{22}(x, y) = \frac{1 + 0.5x + y}{12}, \quad k_{12}(x, y) = k_{21}(x, y) = 0. \tag{3.20}$$

Figure 2 displays the contour lines of constant temperature (isotherms) at various snapshots $t \in \{0.10, 0.20, 0.40, 1.0\}$.

4 Nonlinear optimization of the inverse problem

Notice that if $\mathbf{K}$ is unknown the problem (2.1)-(2.7) is an ill-posed problem and additional information should be added. The overspecified data is given from the measurement, which in this study is assumed to be given by the interior temperatures

$$u(x_i, y_j, t_n) = U^n_{i,j}, \quad i = \overline{1, n_x},\ j = \overline{1, n_y},\ n = \overline{1, n'_t}, \tag{4.21}$$

where n'_t represents the number of instants at which the measurements are recorded and it can vary from 1 to n_t. It is not necessary that the locations (x_i, y_j) and the times t_n coincide with the nodes of the FDM mesh, but we consider so for simplicity. In computation, the data (4.21) is numerically simulated by solving first the direct problem with known conductivity $\mathbf{K}$, as described in the previous section.

This inverse formulation is similar to the aquifer identification problem investigated by Yakowitz and Duckstein (1980) which consists of estimating the transmissivity $\mathbf{K}(x, y)$ from the piezometric head noisy observations (4.21) at the wells (x_i, y_j) and sampling times t_n. Also, a similar formal identification of isotropic conductivity on the basis of internal temperature data measured at a single time step, say $u(x_i, y_j, t_1)$, or at the steady state, $u(x_i, y_j, t_\infty)$ has been described in Carrera and Neuman (1986a).

The determination of optimal locations (x_i, y_j) and times t_n of measurements (4.21) belongs to the area of network design, see e.g. Carrera and Neuman (1986b), and is beyond the scope of this paper. We look however, at how increasing the number of time measurements n'_t from 1 to n_t improves the accuracy of the numerical solution.

The number of unknowns in the inverse problem (2.1), (2.3)-(2.8) and (4.21) is $n_x n_y$ and $2n_x n_y$ in the isotropic and orthotropic cases, respectively, while the number of measurements is $n_t' n_x n_y$. Since in general n_t' is much greater than 3 the identification problem is greatly overdetermined and hence we expect a unique solution. We should also mention here the very interesting work of Huang and Chin (2000) who considered recovering an isotropic both space- and time-dependent conductivity from the full internal temperature data (4.21) with $n_t' = n_t$.

The unknown thermal conductivity in the model is estimated in such a way that the following regularized least squares objective function is minimized:

$$\min J(\mathbf{K}) = \sum_{n=1}^{n_t'} \sum_{i=1}^{n_x} \sum_{j=1}^{n_y} \left(u_{i,j}^n(\mathbf{K}) - U_{i,j}^n\right)^2 + \lambda \sum_{i=1}^{n_x} \sum_{j=1}^{n_y} \|\mathbf{K}(x_i, y_j)\|^2, \tag{4.22}$$

where $\lambda \geq 0$ is a regularization parameter to be prescribed and $u_{i,j}^n$ is the computed temperature obtained from the solution of the direct problem (3.10)-(3.15) at each iteration. In the second term of (4.22) the norm is computed as $\|\mathbf{K}(x_i, y_j)\|^2 = k_{11}^2(x_i, y_j) + k_{22}^2(x_i, y_j)$. Incorporating the regularization term in (4.22) eliminates the effects of non-identifiability of the solution's instability, see e.g. Cooley (1982).

Several Matlab toolbox solvers are available for minimizing various types of objective functions, e.g. **lsqnonlin**, **fmincon**. These toolboxes depend on several algorithms, e.g. trust-region-reflective, Levenberg-Marquardt, interior-point and others which can be used according to the minimization problem under consideration. It is also worth mentioning here the conjugate gradient method (CGM) of Alifanov (1974), see Jarny et al. (1991), whose numerical implementation for the isotropic case was undertaken by Huang and Chin (2000), but its extension to anisotropic heterogenous conductivity identification is yet to be performed. This will be the subject of future work.

For minimizing (4.22) in our problem, we suggest to use the **lsqnonlin** which is designed for linear and nonlinear constrained minimization of a sum of squares. It depends on trust-region-reflective algorithm [4, 8], based on the idea that the region is extended in case that the objective function is well-approximated otherwise, is contracted.

5 Numerical experiments

In this section, we solve the inverse problem iteratively for simultaneously estimating the unknown thermal conductivity $\mathbf{K}(x, y)$. We will illustrate the behavior and the convergence of the iterative minimization for functional (4.22) in terms of the number of iterations using the routine **lsqnonlin**. Before embracing the numerical experiments it is worth mentioning that the most challenging problem in the identification is how to treat the error or the noise in the measurements. Therefore, the interplay between the noise and regularization is crucial in order to obtain a stable and accurate solution.

5.1 Example 1: Isotropic thermal conductivity

In this example we consider the problem (2.1)-(2.7) and (4.21) with unknown isotropic scalar function $k_{11}(x, y) = k_{22}(x, y) = K(x, y)$. The data in (4.21) is numerically simulated and

obtained by solving first the direct problem (2.1)-(2.7) with the zero initial temperature (3.17), the heat flux specification (3.18) and the thermal conductivity (3.19). Snapshots of which have been illustrated in Figure 1. In the inverse analysis we take the initial guess

$$k_{11}^0(x,y) = 1/12 \tag{5.23}$$

and solve the inverse problem (2.1)-(2.7) and (4.21) iteratively by minimizing the regularized least squares functional (4.22) from the initial guess (5.23), as described in Section 4. Simple bounds on the conductivity $k_{11}(x,y)$ are specified as the lower and upper limits 0 and $\max_{(x,y)\in\bar{\Omega}} |k_{11}^0(x,y)| = 1/4$, respectively. This way we ensure that during the iteration procedure the explicit FDM described in Section 3 is always stable, see criterion (3.16).

The convergence of the functional (4.22), as a function of the number of iterations, is shown in Figure 3(a). From this figure, it can be seen that only a few iterations ensure the convergence of the objective function. Figure 3(b) illustrates the comparison between the exact and the estimated conductivity values and very good agreement can be observed.

Next, we add noise to the direct problem solution, as follows:

$$U_{i,j}^n = u(x_i, y_j, t_n) + \varepsilon_{i,j,k}, \quad i = \overline{1, n_x},\ j = \overline{1, n_y},\ n = \overline{1, n_t'}, \tag{5.24}$$

where $\varepsilon_{i,j,k} = normrnd(0, \sigma, n_x n_y n_t')$ are random variables generated from a Gaussian normal distribution with mean zero and standard deviation

$$\sigma = p \times \max\{|u(x,y,t)|; (x,y,t) \in \overline{\Omega} \times [0,T]\}$$

using the Matlab command *normrnd* and p is the percentage of the noise. Adding random noise in (5.24) also ensures that an inverse crime (of using the same data as that generated from the direct solver) is not committed.

Since the inverse problem is ill-posed when we add noise in (5.24) the resulting minimization of the ordinary non-linear least squares functional (4.22) with $\lambda = 0$ will produce an unstable solution. Therefore, in order to overcome this instability we regularize (4.22) by including the positive regularization parameter λ in it.

We estimated the function k_{11} from the noisy temperature measurements (5.24) for various levels of noise $p \in \{1, 2, 3\}\%$. Note that from the numerical implementation for this case we have seen that $n_t' = 3$ is sufficient to yield an accurate and convergent solution.

Figure 4 shows the numerical results for the thermal conductivity obtained with various regularization parameters $\lambda \in \{0, 2, 3, 4, 6\}$ and noise levels $p \in \{1, 2, 3\}\%$. As expected, the numerical results approximate better the exact solution, as the amount of noise p decreases provided that a suitable regularization parameter λ (depending on p) is selected. Generally, the graphs illustrated in Figure 4 reflect the behavior of the numerical solutions for various regularization parameters λ whose choices depend on the amount of noise p with which the data (5.24) is contaminated. In our numerical investigations the appropriate values for the regularization parameter λ have been chosen, for simplicity, by trial and error. This is done by observing the numerical results for several small and large values of λ, gradually increasing and decreasing them until any seemingly unbounded oscillation in the solution obtained has been removed hence, giving a compromise balance between accuracy and stability which is commonly encountered when solving ill-posed problems. Of course, one could also use more

sophisticated criteria for choosing λ such as the L-curve method, see Hansen (2001) or the discrepancy principle, see Morozov (1966). By inspecting Figure 4 one can observe that appropriate values for λ are $\lambda = 2$ or 3 for $p = 1\%$ noise, and $\lambda = 3$ or 4 for $p = 2\%$ and 3% noise. We also remark that the numerical estimates for $p = 2\%$ and 3% are qualitatively similar in behavior.

We finalize this subsection by presenting in Figure 5 the lines of constant $k_{11}(x, y)$. From this figure it can be seen that reasonably stable numerical solutions are obtained when regularization is enforced and that, as expected, the accuracy increases as the level of noise decreases.

5.2 Example 2: Orthotropic thermal conductivity

In this example, we consider an orthotropic planar material whose middle plane is taken as the coordinate system Oxy and the x- and y-axes are coincident with the principal directions of thermal conductivity. Thus, the general tensor (2.2) has the second diagonal equal to zero, i.e. $k_{12} = k_{21}$=0, and is given by (2.8). In the inverse analysis we take the initial guess

$$k_{11}^0(x, y) = k_{22}^0(x, y) = 1/12, \tag{5.25}$$

and try to retrieve the orthotropic tensor (3.20). Note that from the numerical implementation for this case we have seen that $n_t' = 5$ is sufficient to get accurate and convergent numerical solutions. All the other numerical details are the same as those for example 1.

The numerical results for no noise are presented in Figure 6. Compared to Figure 3(a) of the isotropic case, Figure 6(a) shows a larger number of iterations being required to achieve the convergence of the objective function (4.22). This is to be expected because in the orthotropic case we have two functions k_{11} and k_{22} to estimate in comparison with the isotropic case in which only a single function $k_{11} = k_{22}$ is estimated. Even so, the accuracy of the numerical results illustrated in Figures 6(b) and 6(c) is excellent.

Next we investigate the performance of the numerical inversion of noisy data (5.24) contaminated with $p \in \{1, 2, 3\}\%$ noise.

The numerical results for $k_{11}(0.5, y)$ and $k_{22}(0.5, y)$ obtained by inverting $p \in \{1, 2, 3\}\%$ noisy data (5.24) with various regularization parameters $\lambda \in \{0, 0.5, 1.5, 2.0\}$ are illustrated in Figures 7 and 8, respectively. As expected, the results are unstable and inaccurate for $\lambda = 0$, but the stability can be restored through the inclusion of appropriate regularization.

In the next section we consider an application of our study in numerical heat transfer.

6 Cure modelling in composite materials

The model concerns the curing of a carbon fiber reinforced composite in a resin transfer mold (RTM) after the fiber preform has been completely wetted out by the resin. It is a temperature dependent procedure as the reaction changes with temperature. When forced convection does not occur heat conduction is the only heat transfer mechanism relevant to composites cure. The degree of cure, α is generally used to express the resin chemical reaction. Accordingly, the governing equations are given by, see Lim and Lee (2000):

- Thermal model:

$$\rho c_p \partial_t u - \nabla \cdot (K(x,y)\nabla u) = \phi \Delta H \frac{d\alpha}{dt}, \quad (x,y,t) \in \Omega \times (0,T], \tag{6.26}$$

- Kinetic model: The more applied model for a variety of resins is Kamal's model (1974), see also Dusi et al. (1987),

$$\frac{d\alpha}{dt} = \Big(A_1 \exp\Big(\frac{-E_1}{Ru}\Big) + A_2 \exp\Big(\frac{-E_2}{Ru}\Big)\alpha^{m_1}\Big)(1-\alpha)^{m_2}, \quad \alpha(0) = 0, \tag{6.27}$$

where the heat capacity ρc_p and thermal conductivity K, assumed for simplicity to be isotropic, are defined as

$$\rho c_p = \phi \rho_r c_{pr} + (1-\phi)\rho_f c_{pf} \quad \text{and} \quad K = \phi k_r + (1-\phi)k_f,$$

ρ is density, c_p is specific heat, ΔH is heat of reaction, α is the current degree of cure, ϕ is the porosity of the fiber preform, A_1, A_2 are the reaction rate constants, E_1, E_2 are the activation energies, the exponents m_1, m_2 are the reaction orders, where the total reaction order $m_1 + m_2 = 2$, see Michaud et al. (2002), and R refers to the universal gas constant. The subscripts r and f denote the resin and fiber, respectively.

6.1 Numerical approximation

In this section, we describe the FDM used for discretising equations (6.26) and (6.27). This is given by

$$\begin{aligned}\rho c_p(x_i,y_j)\frac{u_{i,j}^{n+1}-u_{i,j}^n}{\tau} &= K_{i,j}\frac{u_{i+1,j}^n - 2u_{i,j}^n + u_{i-1,j}^n}{h_x^2} + K_{i,j}\frac{u_{i,j+1}^n - 2u_{i,j}^n + u_{i,j-1}^n}{h_y^2} \\ &+ (\partial_x K)_{i,j}\frac{u_{i+1,j}^n - u_{i-1,j}^n}{2h_x} + (\partial_y K)_{i,j}\frac{u_{i,j+1}^n - u_{i,j-1}^n}{2h_y} + \phi\Delta H \frac{d\alpha}{dt}(x_i,y_j,t_n),\end{aligned} \tag{6.28}$$

where

$$\begin{aligned}\frac{d\alpha}{dt}(x_i,y_j,t_n) &= \frac{\alpha_{i,j}^{n+1}-\alpha_{i,j}^n}{\tau} \\ &= \Big(A_1 \exp\Big(-\frac{E_1}{Ru_{i,j}^n}\Big) + A_2 \exp\Big(-\frac{E_2}{Ru_{i,j}^n}\Big)(\alpha_{i,j}^n)^{m_1}\Big)(1-\alpha_{i,j}^n)^{m_2}.\end{aligned} \tag{6.29}$$

These equations are solved with the boundary and initial conditions (3.11)-(3.15). We have performed some numerical simulations for the cure model parameters given in Table 1. The numerical results for the degree of cure obtained by solving the direct problem with the FDM mesh size $h_x = h_y = 0.1$ and the time step $\tau = 2$ minutes for the isotropic constant conductivity $K = 0.5372 W/m\text{K}$ and $T = 15$ hours are shown in Figure 9. The initial temperature (2.7) has been varied for $u_0 \in \{30^o\text{C}, 40^o\text{C}, 50^o\text{C}\}$. This figure indicates that as u_0 increases the profiles for the degree of the cure (and also for temperature - not illustrated for brevity) are getting steeper.

We consider next the identification of the thermal conductivity K as well as the cure degree parameters m_1, A_2 and E_2/R which are assumed unknown; note that it not necessary to retrieve A_1 as the second term in (6.27) is nearly zero. In this case, the objective functional (4.22) will depend on all these unknown parameters to read as

$$\min J(K, A_2, \frac{E_2}{R}, m_1) = \sum_{n=1}^{n'_t} \sum_{i=1}^{n_x} \sum_{j=1}^{n_y} \left(u^n_{i,j}(K, A_2, \frac{E_2}{R}, m_1) - U^n_{i,j} \right)^2 + \lambda \sum_{i=1}^{n_x} \sum_{j=1}^{n_y} \|K(x_i, y_j)\|^2. \tag{6.30}$$

The upper and lower bounds for the unknowns $(K(x_i, y_j))_{i=\overline{1,n_x}, j=\overline{1,n_y}}$, m_1, A_2 and E_2/R have been taken as $0.1 \leq K(x_i, y_j) \leq 1.5$ for $i = \overline{1, n_x}$, $j = \overline{1, n_y}$, $0.2 \leq m_1 \leq 0.8$, $1.0 \times 10^{10} \leq A_2 \leq 4.0 \times 10^{11}$ and $0.94 \times 10^5 \leq E_2/R \leq 10^5$. The initial guesses for the unknowns were taken to be $K^0(x_i, y_j) = 0.1$ for $i = \overline{1, n_x}$, $j = \overline{1, n_y}$, $m_1^0 = 0.2$, $A_2^0 = 1.0 \times 10^{10}$ and $(E_2/R)^0 = 0.94 \times 10^5$. We also take $n_x = n_y = 10$, $\tau = 2$ minutes, $T = 15$ hours and $n_t = n'_t = 450$. Table 2 shows an excellent agreement being obtained between the numerical and exact values of these parameters. Furthermore, Figure 10 illustrates the good accuracy and stability of the numerical solution for the isotropic thermal conductivity for both exact and noisy data.

7 Conclusion

The identification of the heterogeneous and orthotropic thermal conductivity which may also include constant unknown parameters related to the degree of cure has been undertaken. The proposed inversion method was based on the penalised least-squares minimization of the sum of squares of differences between the measured and the calculated (by the FDM) internal temperatures in both space and time. Numerically, this was accomplished using the Matlab toolbox routine **lsqnonlin**. Numerical results show high accuracy for exact data and reasonable stability when noisy data are inverted. Physical insight and significance has been further added by considering a cure modelling application in numerical heat transfer. Future work will consist of extensions to three dimensions.

References

[1] O.M. Alifanov, Solution of an inverse problem of heat conduction by iteration methods, J. Eng. Phys. 26 (4) (1974) 471-476.

[2] O.M. Alifanov, Inverse problems in identification and modeling of thermal processes: Russian contributions, Int. J. Numer. Meth. Heat Fluid Flow 27 (3) (2017) 711-728.

[3] G. Bal, C. Guo and F. Monard, Inverse anisotropic conductivity from internal current densities, Inverse Problems 30 (2014) 025001 (21pp).

[4] R.H. Byrd, J.C. Gilbert and J. Nocedal, A trust region method based on interior point techniques for nonlinear programming, Math. Program. 89 (2000) 149-185.

[5] J. Carrera and S.P. Neuman, Estimation of aquifer parameters under transient and steady-state conditions: 2. Uniqueness, stability and solution algorithms, Water Resour. Res. 22 (1986a) 211-227.

[6] J. Carrera and S.P. Neuman, Estimation of aquifer parameters under transient and steady-state conditions: 3. Application to synthetic and field data, Water Resour. Res. 22 (1986b) 228-242.

[7] B. Chen, W. Chen, A.H.-D. Cheng, L.-L. Sun, X. Wei and H. Peng, Identification of the thermal conductivity coefficients of 3D anisotropic media by the singular boundary method, Int. J. Heat Mass Transfer 100 (2016) 24-33.

[8] T.F. Coleman and Y. Li, An interior trust region approach for nonlinear minimization subject to bounds, SIAM J. Optim. 6 (1996) 418-445.

[9] R.L. Cooley, Incorporation of prior information of parameters into nonlinear regression ground water flow models, 1. Theory, Water Resour. Res. 18 (4) (1982) 965-976.

[10] M. Dawson, D. Borman, R.B. Hammond, D. Lesnic and D. Rhodes, A meshless method for solving a two-dimensional transient inverse geometric problem, Int. J. Numer. Meth. Heat Fluid Flow 23 (5) (2013) 790-817.

[11] M.R. Dusi, W.I. Lee, P.R. Ciriscioli and G.S. Springer, Cure kinetics and viscosity of fiberite 976 resin, J. Composite Materials 21 (1987) 243-261.

[12] T.R. Ginn, J.H. Cushman and M.H. Houch, A continuous-time inverse operator for groundwater and contaminant transport modeling: deterministic case, Water Resour. Res. 26 (2) (1990) 241-252.

[13] P.C. Hansen, The L-curve and its use in the numerical treatment of inverse problems, in: P. Johnston (Ed.), Computational Inverse Problems in Electrocardiology, WIT Press, Southampton, 2001, pp. 119-142.

[14] S.D. Harris, R. Mustata, L. Elliott, D.B. Ingham and D. Lesnic, Numerical identification of the hydraulic conductivity of composite anisotropic materials, Computer Modeling Eng. Sci. 25 (2008) 69-79.

[15] M.R. Hematiyan, A. Khosravifard and Y.C. Shiah, A novel inverse method for identification of 3D thermal conductivity coefficients of anisotropic media by the boundary element analysis, Int. J. Heat Mass Transfer 89 (2015) 685-693.

[16] C.-H. Huang and S.-C. Chin, A two dimensional inverse problem in imaging the thermal conductivity of a non-homogeneous medium, Int. J. Heat Mass Transfer 43 (2000) 4061-4071.

[17] D.L. Hughson and A. Gutjahr, Effect of conditioning randomly heterogeneous transmissivity on temporal hydraulic head measurements in transient two-dimensional aquifer flow, Stochastic Hydrol. Hydraul. 12 (1998) 155-170.

[18] S. Irmay, Piezometric determination of inhomogenoeus hydraulic conductivity, Water Resour. Res. 16 (4) (1980) 691-694.

[19] Y. Jarny, M.N. Ozisik and J.P. Bardon, A general optimization method using adjoint equation for solving multidimensional inverse heat conduction, Int. J. Heat Mass Transfer 34 (11) (1991) 2911-2919.

[20] M.R. Kamal, Thermoset characterization for moldability analysis, Polymer Engineering Sci. 14 (1974) 231-239.

[21] I. Knowles, Parameter identification for elliptic problems, J. Comput. Appl. Math. 31 (2001) 175-194.

[22] I. Knowles and A. Yan, The recovery of an anisotropic conductivity in groundwater modelling, Appl. Anal. 81 (2002) 1347-1365.

[23] R. Kohn and M. Vogelius, Determining conductivity by boundary measurments. II Interior results, Comm. Pure Appl. Math. 38 (1985) 643-667.

[24] D. Lesnic, R. Mustata, B. Clennell, L. Elliott, S.D. Harris and D.B. Ingham, Genetic algorithm to identify the hydraulic properties of heterogeneous rocks from laboratory flow-pump experiments, J. Porous Media 10 (2007) 71-91.

[25] S.T. Lim and W.I. Lee, An analysis of the three-dimensional resin-transfer mold filling process, Composites Science and Technology 60 (2000) 961-975.

[26] W.R.B. Lionheart, Conformal uniqueness results in anisotropic electrial impedance imaging, Inverse Problems 13 (1997) 125-134.

[27] D.J. Michaud, A.N. Bres and P.S. Dhurjati, Thick-section RTM composite manufacturing: Part I in-situ cure model parameter identification and sensing, J. Composite Materials 36 (2002) 1175-1199.

[28] V. Monchiet and G. Bonnet, A polarization-based fast numerical method for computing the effective conductivity of composites, Int. J. Numer. Meth. Heat Fluid Flow 23 (7) (2013) 1256-1271.

[29] V.A. Morozov, On the solution of functional equations by the method of regularization, Sov. Math. Dokl. 7 (1966) 414-417.

[30] R. Mustata, S.D. Harris, L. Elliott, D. Lesnic, D.B. Ingham, R.A. Khachfe and Y. Jarny, The determination of the properties of orthotropic heat conductors, In: Inverse Problems and Experiemental Design in Thermal and Mechanical Engineering, (eds. D. Petit, D.B. Ingham, Y. Jarny and F. Plourde), Proceedings of the Eurotherm Seminar 68, March 5-7, 2001, Poitiers, France, pp. 325-332.

[31] M.N. Ozisik, Heat Conduction, John Wiley and Sons, Inc, New York, 1993.

[32] M. Paruch, Identification of the cancer ablation parameters during RF hyperthermia using gradient, evolutionary and hybrid algorithms, Int. J. Numer. Meth. Heat Fluid Flow 27 (3) (2017) 674-697.

[33] G.R. Richter, An inverse problem for the steady state diffusion equation, SIAM J. Appl. Math. 41 (1981) 210-221.

[34] S. Yakowitz and L. Duckstein, Instability in aquifer identification: theory and case studies, Water Resour. Res. 16 (6) (1980) 1045-1064.

[35] G. Yan, W. Chen, C. Zhang and X. He, A meshless singular boundary method for three-dimensional inverse heat conduction problems in general anisotropic media, Int. J. Heat Mass Transfer 84 (2015) 91-102.

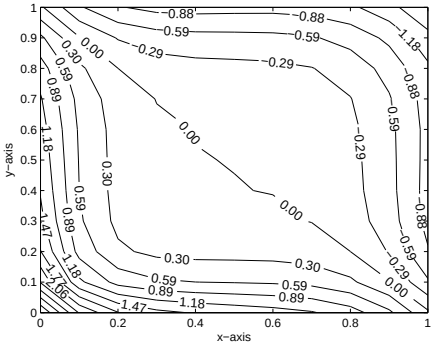

(a) $t = 0.10$

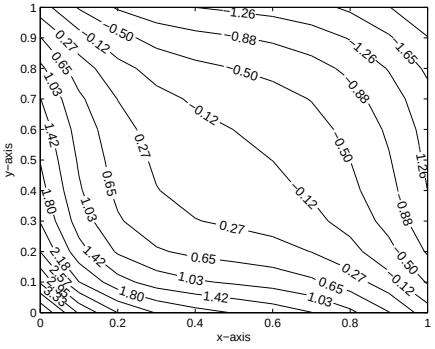

(b) $t = 0.20$

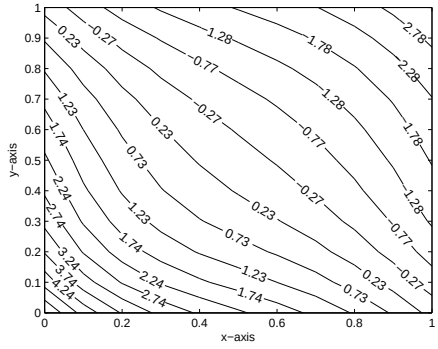

(c) $t = 0.40$

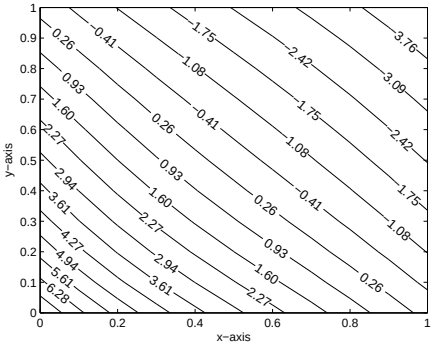

(d) $t = 1$

Figure 1: Isotherms for the direct problem at various snapshots of time $t \in \{0.10, 0.20, 0.40, 1\}$ for the isotropic medium (3.19).

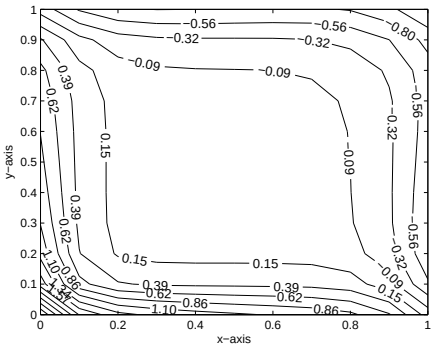

(a) $t = 0.10$

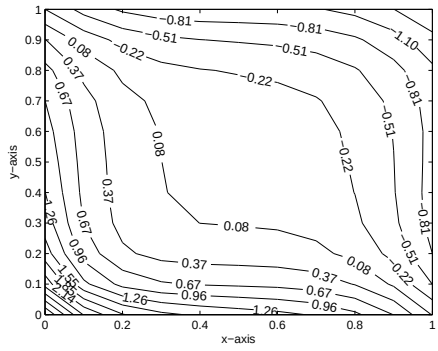

(b) $t = 0.20$

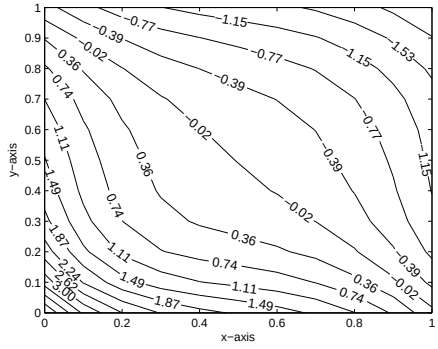

(c) $t = 0.40$

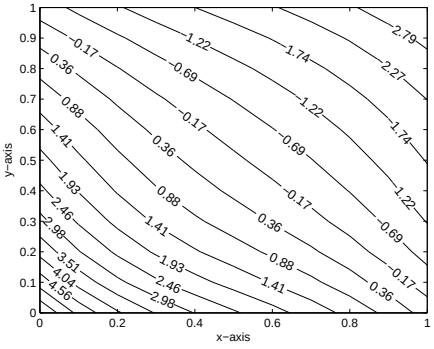

(d) $t = 1$

Figure 2: Isotherms for the direct problem at various snapshots of time $t \in \{0.10, 0.20, 0.40, 1\}$ for the orthotropic medium (3.20).

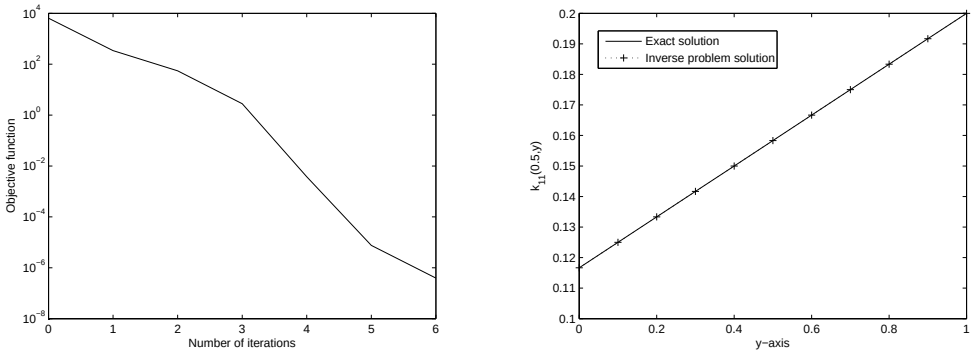

(a) (b)

Figure 3: (a) Unregularized objective function, as a function of the number of iterations, (b) Retrieved and exact isotropic thermal conductivity coefficient k_{11} at $x = 0.5$ with no noise.

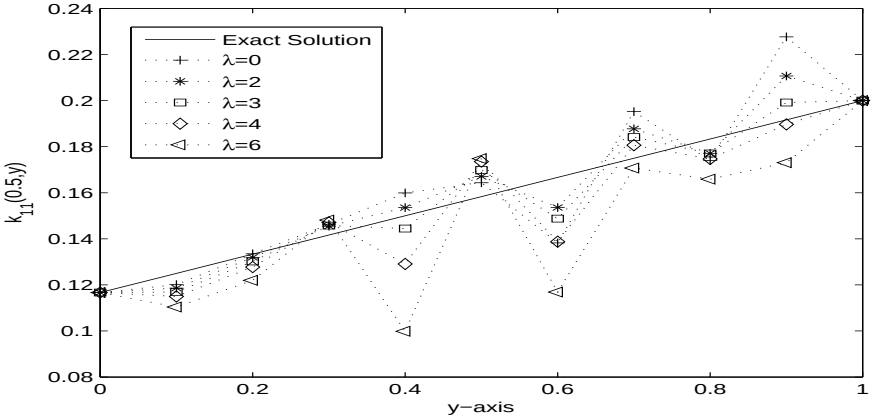

(a)

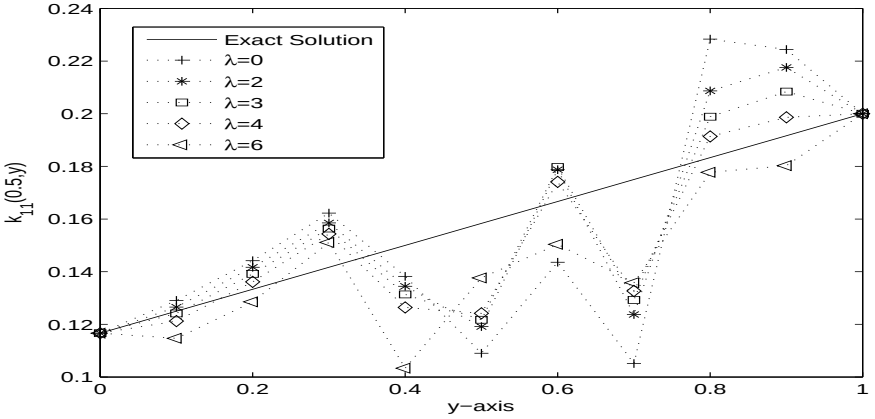

(b)

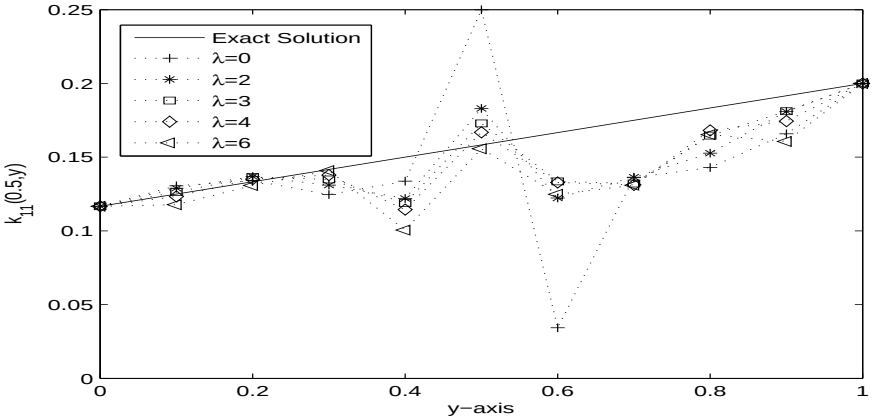

(c)

Figure 4: Thermal conductivity $k_{11}(0.5, y)$ for (a) $p = 1\%$ (b) $p = 2\%$ and (c) $p = 3\%$ noises and various regularization parameters for the isotropic case of example 1.

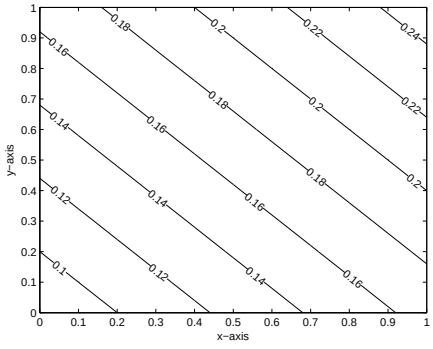

(a) Exact

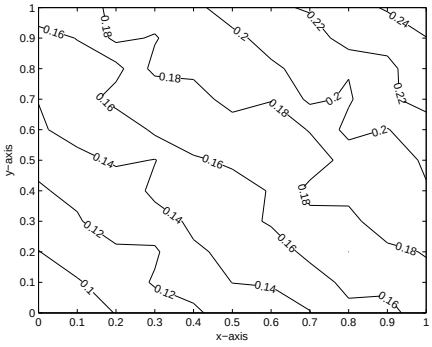

(b) $p = 1\%$ noise with regularization

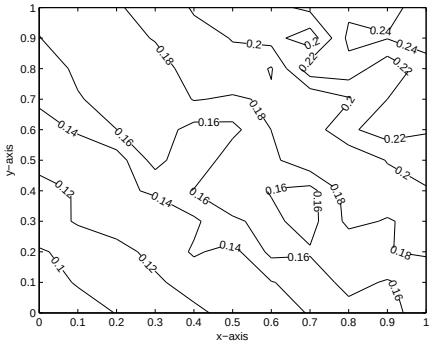

(c) $p = 1\%$ noise without regularization

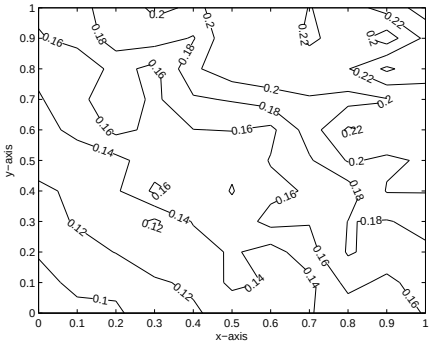

(d) $p = 2\%$ noise with regularization

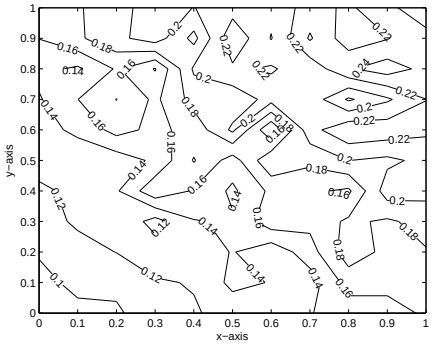

(e) $p = 2\%$ noise without regularization

Figure 5: Lines of constant $k_{11}(x, y)$ for the isotropic case of example 1.

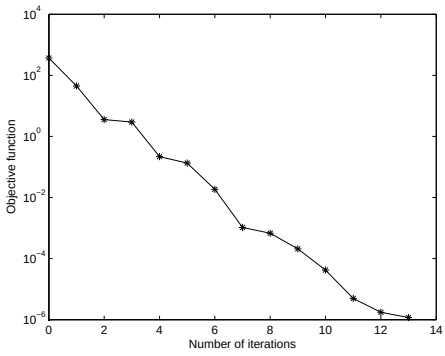

(a)

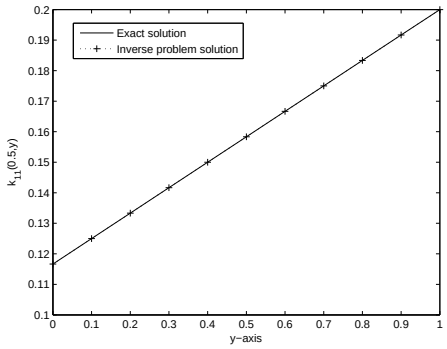

(b)

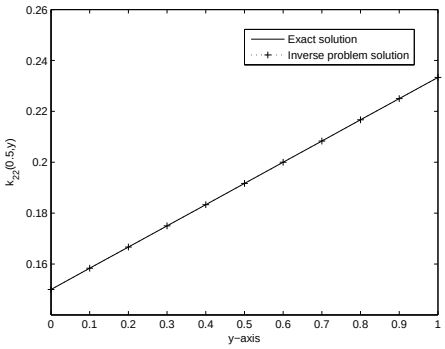

(c)

Figure 6: (a) Unregularized objective function, as a function of number of iterations, (b) and (c) identification of orthotropic thermal conductivity components $k_{11}(0.5, y)$ and $k_{22}(0.5, y)$, respectively, no noise, for example 2.

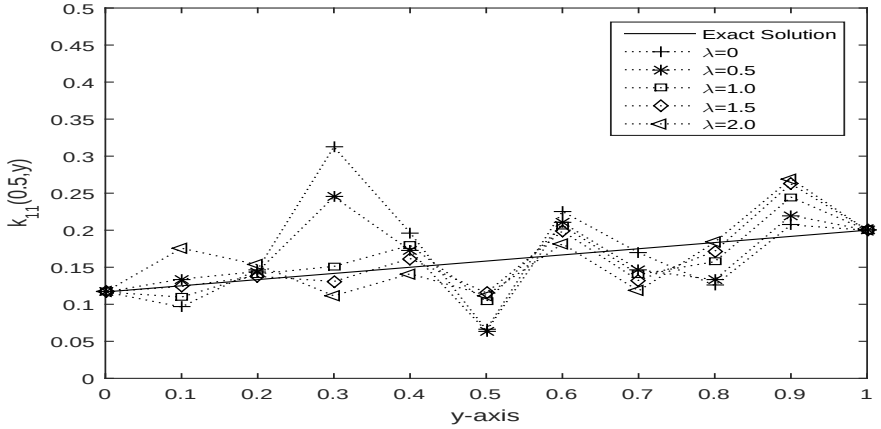

(a)

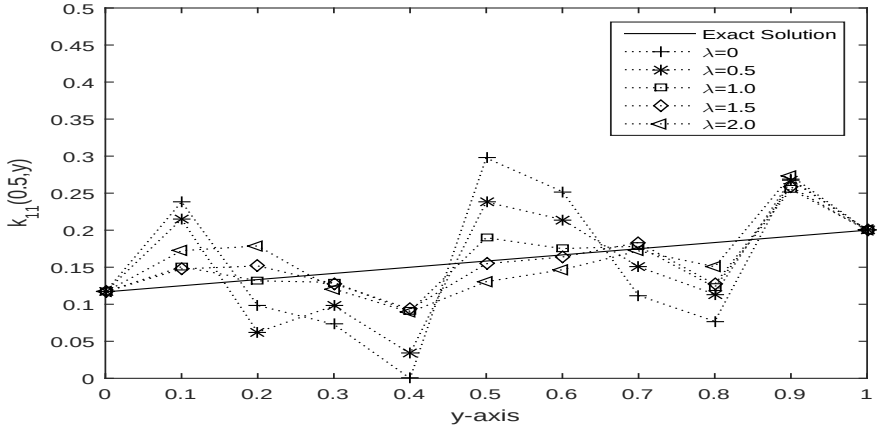

(b)

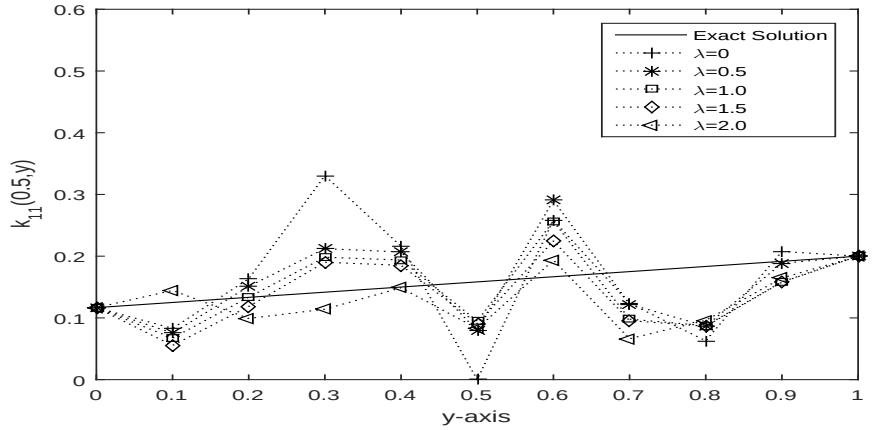

(c)

Figure 7: Thermal conductivity $k_{11}(0.5, y)$ with (a) $p = 1\%$, (b) $p = 2\%$ and (c) $p = 3\%$ noises and various regularization parameters for the orthotropic case of example 2.

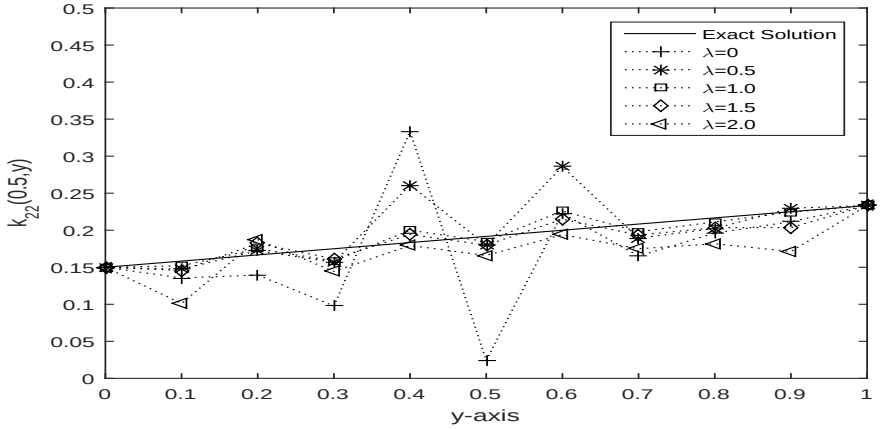

(a)

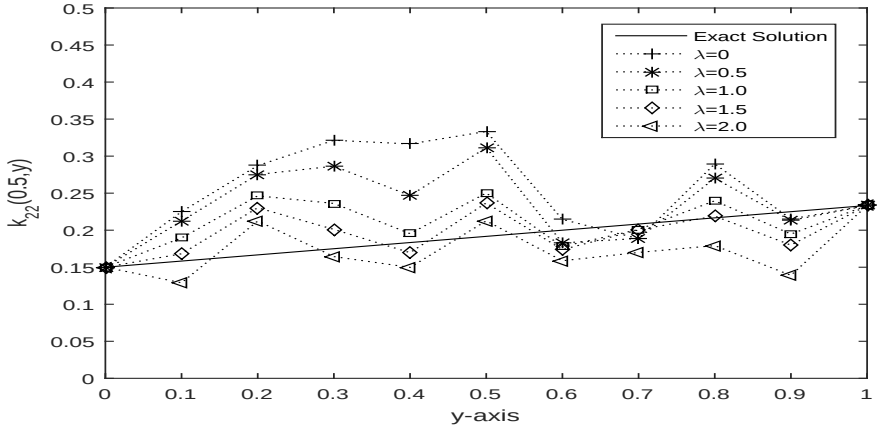

(b)

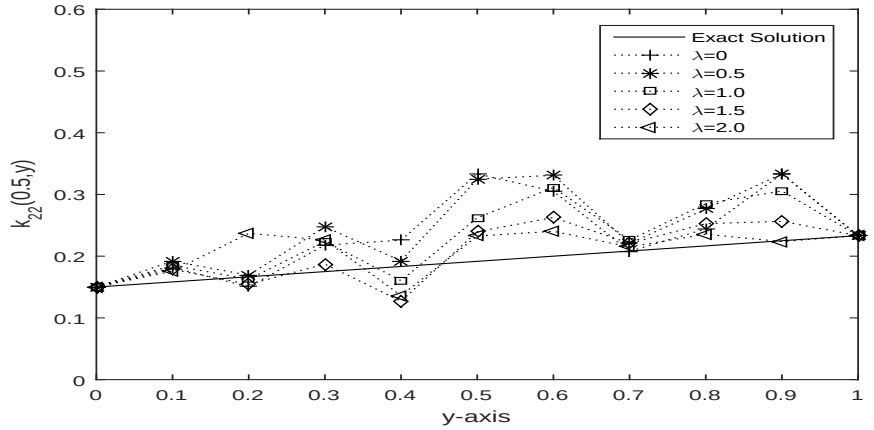

(c)

Figure 8: Thermal conductivity $k_{22}(0.5, y)$ with (a) $p = 1\%$, (b) $p = 2\%$ and (c) $p = 3\%$ noises and various regularization parameters for the orthotropic case of example 2.

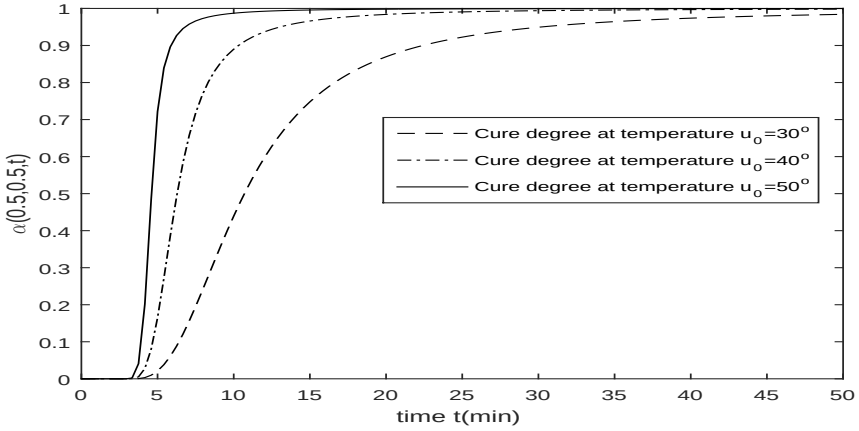

Figure 9: The degree of cure $\alpha(0.5, 0.5, t)$ for various initial temperatures u_0.

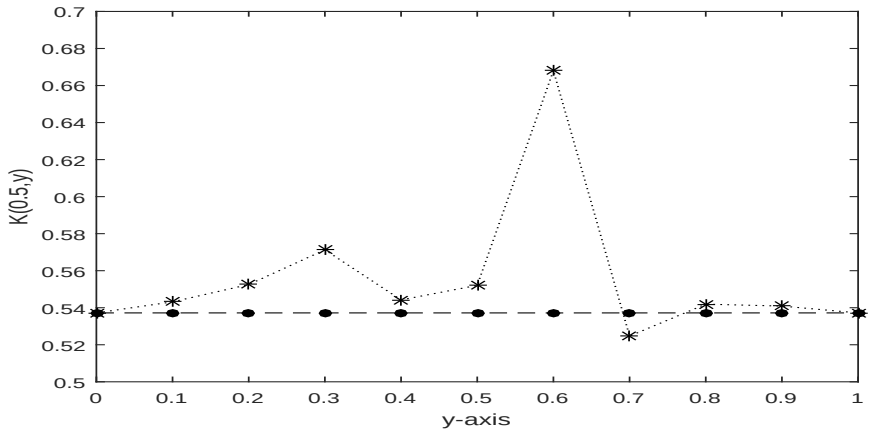

Figure 10: The retrieved thermal conductivity $K(0.5, y)$ of the cure model with no noise ($\bullet$), and with $p = 1\%$ noise and $\lambda = 5 \times 10^{-4}$ $(\cdot * \cdot)$ in comparison with the exact solution $(- - -)$.

Table 1: Cure model parameters from Lim and Lee (2000). We also have $\phi = 0.4$ and $\Delta H = 2.79 \times 10^5 J/kg$ for vinylester.

(Parameters of cure kinetics)						
E_1/R	E_2/R	A_1	A_2	m_1	m_2	
100048.4 K	9480.58 K	1.2483×10^{10} $\min^{-1}$	2.0433×10^{11} $\min^{-1}$	0.693	1.327	
(Parameters of fiber)				(Parameters of resin)		
ρ_f	c_{pf}	k_f		ρ_r	c_{pr}	k_r
2540 kg/m^3	835 J/kgK	0.76 W/mK		1030.4 kg/m^3	1900 J/kgK	0.193 W/mK

Table 2: Parameter identification of the cure model.

	m_1	A_2	E_2/R
Exact	0.6930	2.0433×10^{11}	9.4807×10^3
$p = 0$	0.6930	2.0433×10^{11}	9.4807×10^3
$p = 1\%$	0.6960	2.0433×10^{11}	9.4766×10^3